Monthly Notices
of the
ROYAL ASTRONOMICAL SOCIETY

Mon. Not. R. Astron. Soc. **422,** 812–818 (2012) doi:10.1111/j.1365-2966.2012.20660.x

Hyperfine collisional rate coefficients of CN with $H_2(j = 0)$

Yulia Kalugina,[1,2] François Lique[1⋆] and Jacek Kłos[3]

[1]*LOMC – UMR 6294, CNRS-Université du Havre, 25 rue Philippe Lebon, BP 540, 76058 Le Havre, France*
[2]*Department of Optics and Spectroscopy, Tomsk State University, 36 Lenin Avenue, Tomsk 634050, Russia*
[3]*Department of Chemistry and Biochemistry, University of Maryland, College Park, MD 20742, USA*

Accepted 2012 January 31. Received 2012 January 29; in original form 2012 January 2

ABSTRACT

Modelling of molecular emission spectra from interstellar clouds requires the calculation of rate coefficients for excitation by collisions with the most abundant species. Among the interstellar molecules, the CN radical is of particular interest since it is a good probe of dense region and can be used as a tracer of magnetic fields. We calculate fine- and hyperfine-structure-resolved excitation rate coefficients of $CN(X^2\Sigma^+)$ by $H_2(j = 0)$, the most abundant collisional partner in the interstellar medium. The calculations are based on a new potential energy surface obtained from highly correlated ab initio calculations. State-to-state rate coefficients between the first fine and hyperfine levels of CN were calculated for low temperatures ranging from 5 to 100 K. The new results are compared to the CN–He rate coefficients. Significant differences are found between the two sets of rate coefficients. This comparison shows that the CN–H_2 rate coefficients have to be used for observation interpretations and we expect that their use will significantly help the astronomers in the interpretation of the CN emission lines observed with current and future telescopes.

Key words: molecular data – molecular processes – scattering.

1 INTRODUCTION

The cyano radical (CN) molecule is one of the most widely distributed in the interstellar medium (ISM). CN was the second interstellar molecule to be identified, going back to the 1940s (McKellar 1940; Adams 1941). Since then, CN has been extensively observed (Fuente, Martin-Pintado & Gaume 1995; Falgarone et al. 2008; Hily-Blant et al. 2008; Milam, Woolf & Ziurys 2009; Hakobian & Crutcher 2011). In diffuse molecular gas, CN plays a role as a tracer of high-density gas. The CN thermal lines also probe dense regions in molecular clouds and CN Zeeman observations are a unique tool for measuring magnetic field strengths in star formation regions (Falgarone et al. 2008). In addition, the triple bond between C and N leaves one electron available in the CN radical that makes CN a very reactive molecule. Reactions between CN and unsaturated hydrocarbons like acetylene and ethylene have been shown to be efficient even at very cold temperatures (Balucani et al. 2000). Organic molecules with the CN group are known as nitriles. They are potential source of prebiotic amino acids.

The existence of accurate collisional rate coefficients for CN is thus crucial to the interpretation of CN molecular line observations and hence having a good knowledge of the CN abundance and chemistry in the ISM. Without these rates, only approximate estimates of the molecular abundance are possible assuming local thermodynamic equilibrium, which at the typical densities of dense interstellar clouds is generally not a good approximation for such a molecule (Lique et al. 2009).

The determination of rate coefficients for collisions between CN molecule and the most abundant interstellar species has been one of the important goals of molecular astrophysics in past decades. Indeed, CN rate coefficients have been tentatively estimated from a scaling of the CO or CS rate coefficients (Truong-Bach et al. 1987; Fuente et al. 1995) but the scaling from CO or CS fails because CN is an open shell molecule and has a $^2\Sigma^+$ ground state. The first realistic CN rate coefficients have only been provided during the last two years. Accurate CN–He rate coefficients taking into account the fine and hyperfine structure of CN have been provided by Lique et al. (2010) and Lique & Kłos (2011). Rate coefficients between the first 41 fine-structure levels of CN in collisions with He have been calculated by Lique et al. (2010) for temperature ranging from 5 to 350 K. These calculations were extended to the CN hyperfine structure by Lique & Kłos (2011). These first rate coefficients for the CN molecule enable a more realistic determination of CN distribution in molecular clouds. However, the collisional partner was the He atom and recent results on rotational excitation of CO (Wernli et al. 2006), SiS (Kłos & Lique 2008; Lique & Kłos 2008) or HF (Guillon & Stoecklin 2012) have pointed out that rate coefficients for collisions with $H_2(j = 0)$, the most abundant collisional partner in the ISM, are generally different from those for collisions with He.

Taking into account the importance of having accurate rate coefficients for the CN–H_2 collisional system, we have decided to extend the calculations of Lique et al. (2010) and Lique & Kłos (2011), both of the potential energy surface (PES) and of the

⋆E-mail: francois.lique@univ-lehavre.fr

inelastic cross-sections, to the CN–H_2 system. The collision between a CN radical and H_2 has been the subject of many studies (Ter Horst, Schatz & Harding 1996; Coletti & Billing 2000; Zhang & Lee 2000). However, all these works were only focused on reactive collisions and in the formation of HCN molecule. Most of these calculations were based on the TSH3 PES (Ter Horst et al. 1996). This PES, as well as another PES obtained more recently by Kaledin, Heaven & Bowman (1999), was calculated using configuration interaction methods. In this work, we are only interested in the rotational excitation of CN by H_2; therefore, we have decided to determine a new ab initio PES using the 'coupled clusters' approach that has been shown to be more accurate than configuration interaction methods for the van der Waals system well described by a single electronic configuration.

The determination of rate coefficients for collisions of open shell molecules with diatomic molecules remains a challenge for molecular physics. Hence, we have decided, as a first step, to restrict to calculations with only para-$H_2(j = 0)$. Indeed, the calculations with $H_2(j = 0)$ can be performed using a PES averaged over H_2 rotations. The scattering problem is hence reduced to the study of the collision between a molecule and a structureless target (Lique et al. 2008). These calculations have been shown to be accurate (Lique et al. 2008; Dumouchel, Kłos & Lique 2011) for low-temperature excitation rate coefficients.

The paper is organized as follows. Section 2 describes the ab initio calculation of the PES. Section 3 then provides a brief description of the theory and the calculations. In Section 4, we present and discuss our results. Conclusions of this work are drawn in Section 5.

2 POTENTIAL ENERGY SURFACE

In the present work, we focus on low/moderate-temperature collisions. The CN–H_2 collisional system is a reactive system. The collision of a CN radical with an H_2 molecule can lead to the formation of the two HCN/HNC isomers (Agúndez et al. 2010). However, it has been shown that the reaction was not efficient at typical temperature of the cold ISM (Ter Horst et al. 1996), since the reaction has to proceed through a large barrier. The activation energy of the reaction is at least 1100 cm^{-1} (Ter Horst et al. 1996). Then, as it has been shown recently by Lique & Faure (2012) in the case of collisions between H and D_2, the study of the rotational excitation of CN by H_2 can certainly be performed neglecting the reactive pathways. Hence, for the calculation of a CN–H_2 PES for only the rotational excitation, the collision partners may thus be considered as rigid.

The calculation of the CN–H_2 PES will be presented elsewhere. We just present here a brief description of the ab initio calculations. The body-fixed Jacobi coordinate system used in calculations is presented in Fig. 1. The geometry of the CN–H_2 complex is characterized by three angles θ, θ' and φ, and the distance R between the centres of masses of H_2 and CN. The polar angles of the CN and H_2 molecules with respect to z-axis that is defined to coincide with $\boldsymbol{R}$ are denoted, respectively, θ and θ', while φ denotes the dihedral angle, which is the relative polar angle between half-planes containing the CN and H_2 bonds, respectively.

We used an H_2 bond distance $r_{H-H} = 1.4487a_0$, corresponding to the molecular distance at its average value in the ground vibrational level of H_2, and a CN bond distance $r_{C-N} = 2.2144a_0$ (Huber & Herzberg 1979), corresponding to the equilibrium distance. The CN–H_2 PES was calculated at the partially spin-restricted coupled cluster with single, double and perturbative triple excitations [RCCSD(T)] level (Knowles, Hampel & Werner 1993, 2000). The

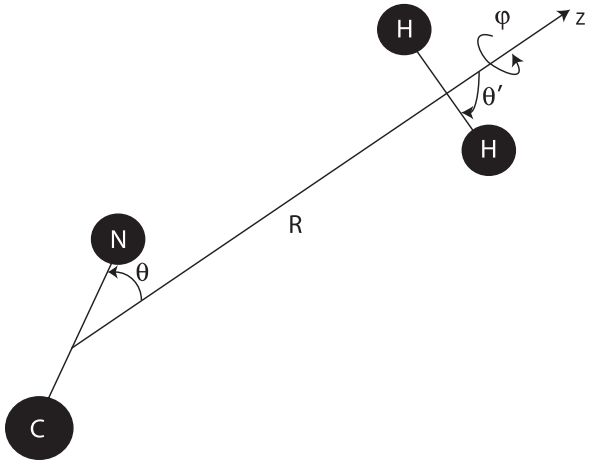

Figure 1. Definition of the body-fixed coordinates system.

four atoms were described by the aug-cc-pVTZ basis set of Woon & Dunning (1994) augmented by the (3s, 2p, 1d) bond functions, defined by Williams et al. (1995), placed at mid-distance between the CN and H_2 centres of mass. The electronic structure calculations were performed using the MOLPRO 2010 package (Werner et al. 2010). In all calculations, to determine the interaction potential $V(R, \theta, \theta', \varphi)$, the basis set superposition error was corrected with the Boys & Bernardi (1970) counterpoise procedure:

$$V(R,\theta,\theta',\varphi) = E_{\mathrm{CN-H_2}}(R,\theta,\theta',\varphi) - E_{\mathrm{CN}}(R,\theta,\theta',\varphi) - E_{\mathrm{H_2}}(R,\theta,\theta',\varphi), \quad (1)$$

where the energies of the CN and H_2 subsystems are computed with the full (four atoms plus bond functions) basis set.

For a van der Waals system, where the ground state is well described by a single predominant configuration at all computed geometries, the RCCSD(T) level of theory and the use of aug-cc-pVTZ basis set augmented by bond functions are expected to yield reliable results (Lique & Kłos 2008).

The radial scattering coordinate R was assigned from $16.0a_0$ to $4.0a_0$, the θ grid ranged from 0° to 180° in steps of 15°, whereas θ' and φ ranged from 0° to 180° and 0° to 90°, respectively, in 22°.5 increment. In the global fitting procedure, we took into account the long-range ab initio points of the potential up to $R = 12a_0$ due to the appearance of geometries with non-convergence in the electronic structure calculations, thus appearance of small unphysical non-smooth irregularities in the radial dependence of the potential.

For the solution of the close-coupling scattering equations, it is most convenient to expand, at each value of R, the interaction potential $V(R, \theta, \theta', \phi)$ in angular functions. For the scattering of two linear rigid rotors, we used the following expansion (Green 1975):

$$V(R,\theta,\theta',\phi) = \sum_{l,l';\mu} v_{l,l';\mu}(R) s_{l,l';\mu}(\theta,\theta',\phi). \quad (2)$$

The basis functions $s_{l,l';\mu}(\theta, \theta', \phi)$ are products of associated Legendre functions P_{lm}:

$$s_{l,l';\mu}(\theta,\theta',\phi) = \left(\frac{2l+1}{4\pi}\right)^{1/2} \left\{ \sum_m (-)^m (2-\delta_{m0}) \langle l m l' -m \mid l l' \mu 0\rangle P_{lm}(\theta) P_{l'm}(\theta') \cos(m\phi) \right\}, \quad (3)$$

where $\langle \ldots | \ldots \rangle$ is a Clebsch–Gordan coefficient. The P_{lm} functions are related to spherical harmonics through $Y_{lm}(\theta, \phi) = P_{lm}(\theta)e^{(im\phi)}$. Here l, l' are associated, respectively, with the rotational motion of CN and H_2. In equation (2), the homonuclear symmetry of H_2 forces the index l' to be even.

We find similar global and local minima as Kaledin et al. (1999) in their work on the H_2–CN(X) PES. Positions of minima on our 4D PES are located slightly closer and generally 20 cm^{-1} deeper in comparison to Kaledin's PES. We will present full features and comparisons between these two 4D potentials in our future work on 4D scattering for this system.

In this work, we only consider the collisional excitation of CN by para-H_2. For collisions at low temperature ($T \leq 100$ K), the rotational excitation probability of H_2 is low (Kłos & Lique 2008; Dumouchel et al. 2011), the energy spacing between the $j = 0$ and 2 levels in para-H_2 being 510 K. Hence, we restrict H_2 to its lowest rotational level and, in this case, only the leading term $l' = \mu = 0$ needs to be retained in the expansion of the interaction potential given in equation (3). The resulting expansion then can be simplified to

$$V_{\rm av}(R, \theta) = \sum_l V_l(R) P_l(\cos\theta), \quad (4)$$

where $V_{\rm av}(R, \theta)$ is obtained by an average over the angular motion $\{\theta', \phi\}$ of the H_2 molecule. The 4D CN–$H_2(j_2 = 0)$ PES is thus reduced to a 2D PES. Finally, the fitting procedure described by Werner et al. (1989) for the CN–He system was adapted in order to obtain the $V_{\rm av}(R, \theta)$ numerical expansion required to perform the scattering calculations. In Fig. 2, we show the contour plot of the interaction energy.

The global minimum of the $V_{\rm av}$ PES occurs for $R = 7.11a_0$ and $\theta = 132.^{\circ}7$, and is of 58.96 cm^{-1} deep. It is interesting to compare this PES with the earlier CN–He PES of Lique et al. (2010). Although the two PES are qualitatively similar, the minimum of the CN–para-$H_2(j = 0)$ PES is three times deeper than that of the CN–He PES. In Fig. 3, we plot the first four radial Legendre expansion coefficients $V_l(R)$ ($\lambda = 0$–3) of the CN–$H_2(j = 0)$ and CN–He PES. We observe that, for the CN–$H_2(j = 0)$ and CN–He system, the largest (in magnitude) of the anisotropic terms ($\lambda > 0$) corresponds to $\lambda = 2$. This implies that, to a first approximation, the PES is symmetric with respect to $\theta \rightarrow \pi - \theta$. One can also see that the CN–$H_2(j = 0)$ radial coefficients are larger in magnitude than those

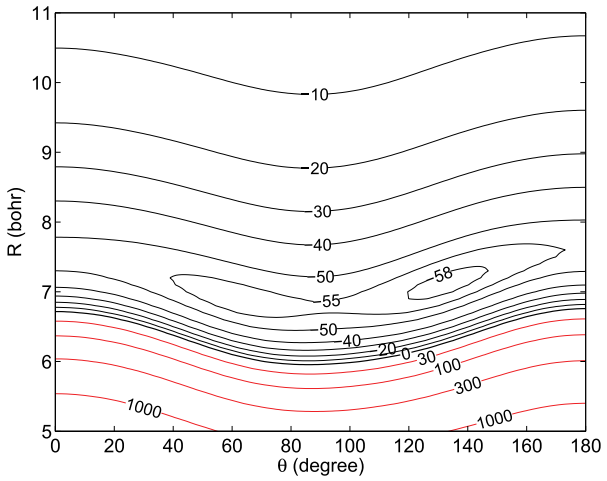

Figure 2. Contour plot of the CN–$H_2(j = 0)$ PES.

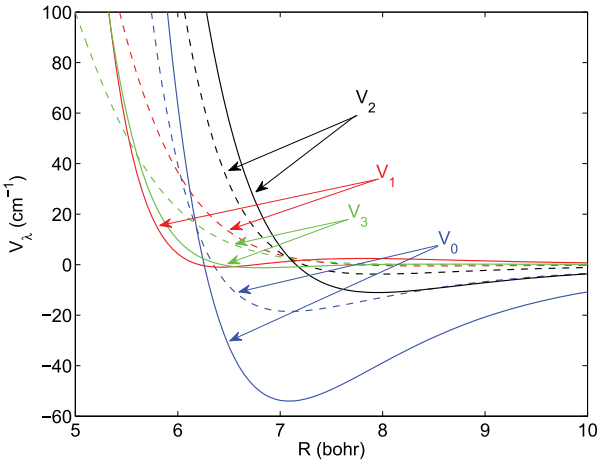

Figure 3. Plot of the first four radial Legendre expansion coefficients ($\lambda = 0 - 3$) as a function of R. Solid lines denote CN–para-$H_2(j = 0)$ while dashed lines denote CN–He.

of the CN–He PES. The consequences for the collisional excitation cross-sections and rate coefficients will be discussed below.

3 SCATTERING CALCULATIONS

The main goal of this work is to use the 2D CN–H_2 PES to determine fine- and hyperfine-resolved integral cross-sections and rate coefficients of CN molecules by $H_2(j = 0)$. As the rotational structure of H_2 is neglected, the problem, in terms of scattering calculations, is equivalent to the collisional excitation of CN by a structureless atom.

For CN in its ground electronic $^2\Sigma^+$ state, the molecular energy levels can be described in the Hund's case (b) limit. Here, the fine structure levels are labelled N_j, where N is the rotational angular momentum and j the total molecular angular momentum quantum number with $\boldsymbol{j} = \boldsymbol{N} + \boldsymbol{S}$, where $\boldsymbol{S}$ is the electronic spin. For molecules in a $^2\Sigma^+$ state, $S = 1/2$. Hence, two kinds of levels exist, the levels with $j = N + 1/2$ and those with $j = N - 1/2$. The nitrogen atom also possesses a non-zero nuclear spin ($I = 1$). The coupling between $\boldsymbol{I}$ and $\boldsymbol{j}$ results in a splitting of each level into three hyperfine levels (except for the $j = 1/2$ level which is split into only two levels). Each hyperfine level is designated by a quantum number F ($\boldsymbol{F} = \boldsymbol{I} + \boldsymbol{j}$) varying between $|I - j|$ and $I + j$.

We used Alexander's description (Alexander 1982) of the inelastic scattering between an atom and a diatomic molecule in a $^2\Sigma^+$ electronic state and a fully quantum close-coupling calculations in order to obtain the $S^J(jl; j'l')$ scattering matrix and integral cross-sections corresponding to an $Nj \rightarrow N'j'$ transition between fine structure levels of CN. J and l denote the total angular momentum ($\boldsymbol{J} = \boldsymbol{j} + \boldsymbol{l}$) and the orbital angular momentum quantum numbers, respectively. The integral cross-sections corresponding to transitions between hyperfine levels of the CN molecule can be obtained from scattering S-matrix between fine structure levels using the recoupling method of Alexander & Dagdigian (1985). Inelastic cross-sections associated with a transition from an initial hyperfine level NjF to a hyperfine level $N'j'F'$ were thus obtained as follow:

$$\sigma_{NjF \rightarrow N'j'F'} = \frac{\pi}{k^2_{NjF}}(2F' + 1)\sum_K \times \begin{Bmatrix} j & j' & K \\ F' & F & I \end{Bmatrix}^2 P^K(j \rightarrow j'). \quad (5)$$

The $P^K(j \to j')$ are the tensor opacities defined by

$$P^K(j \to j') = \frac{1}{2K+1} \sum_{ll'} |T^K(jl; j'l')|^2. \quad (6)$$

The reduced T-matrix elements (where $T = 1 - S$) are defined by Alexander & Davis (1983):

$$T^K(jl; j'l') = (-1)^{-j-l'}(2K+1) \sum_J (-1)^J (2J+1) \times \begin{Bmatrix} l' & j' & J \\ j & l & K \end{Bmatrix} T^J(jl; j'l'). \quad (7)$$

All the scattering calculations were performed with the HIBRIDON package.[1]

Calculations for collision of CN with para-H_2 were carried out for a total energy grid ranging from 0.2 to 1000 cm^{-1}. The integration parameters were chosen to meet convergence criteria of 0.2 per cent for fine-structure-resolved cross-sections. The integration range was set from $4.5a_0$ to $80a_0$. At the largest total energy (1000 cm^{-1}), the CN rotational basis was extended to $j = 17$ to ensure convergence of the first 13 (up to $j = 12$) rotational levels of CN. The maximum value of the total angular momentum J used in the calculations was set to be large enough that the inelastic and 'quasi-elastic' cross-sections were converged.

From the rotationally inelastic cross-sections $\sigma_{NjF \to N'j'F'}(E_c)$, one can obtain the corresponding thermal rate coefficients at temperature T by an average over the collision energy (E_c) (Smith 1980):

$$k_{NjF \to N'j'F'}(T) = \left(\frac{8}{\pi \mu k_B^3 T^3}\right)^{1/2} \times \int_0^\infty \sigma_{NjF \to N'j'F'} E_c \, e^{-E_c/k_B T} \, dE_c, \quad (8)$$

where k_B is Boltzmann's constant and μ is the reduced mass of the CN–H_2 complex.

4 RESULTS

Using the computational scheme described above, we have obtained inelastic (fine and hyperfine) cross-sections up to the total energy of 1000 cm^{-1} for transitions between the first 25 fine levels and the corresponding 76 hyperfine levels of CN ($N, N' \leq 12$). Calculations up to the total energy of 1000 cm^{-1} allow us to determine the corresponding rate coefficients up to 100 K. The complete set of (de-)excitation rate coefficients with $N, N' \leq 12$ is available online at the LAMDA[2] website.

4.1 Fine structure excitation

The variation with temperature of these state-to-state rate coefficients out of the $N, j = 5, 5.5$ rotational level for $\Delta j = \Delta N$ transitions and $\Delta j \neq \Delta N$ transitions is illustrated in Figs 4 and 5.

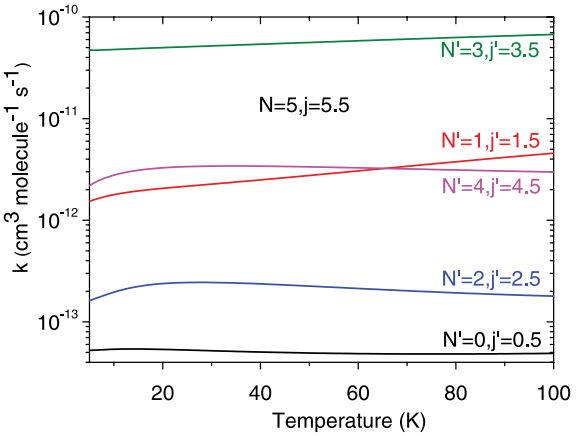

Figure 4. Temperature dependence of CN–$H_2(j = 0)$ rate coefficients for $\Delta j = \Delta N$ transitions out of $N, j = 5, 5.5$ state.

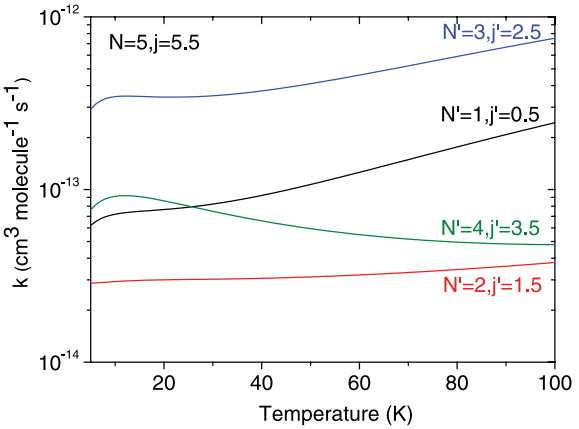

Figure 5. Temperature dependence of CN–$H_2(j = 0)$ rate coefficients for $\Delta j \neq \Delta N$ transitions out of $N, j = 5, 5.5$ state.

We observe a propensity for $\Delta j = \Delta N$ transitions. The same propensity rule was previously obtained for CN–He (Lique et al. 2010). This behaviour, predicted theoretically (Alexander, Smedley & Corey 1986), is a general feature of collisions of molecules in $^{2S+1}\Sigma$ electronic state, as shown previously for the O_2–He collisions (Lique 2010) or SO–H_2 (Lique et al. 2007).

We note in Figs 4 and 5 a strong propensity for transitions with even ΔN. Transitions with $\Delta N = 4$ are even larger than transitions with $\Delta N = 1$. This is a consequence of the near-homonuclear symmetry of the PES that strongly favours transitions with even ΔN. This effect is well known experimentally and was first explained by McCurdy & Miller (1977).

4.2 Hyperfine structure excitation

Fig. 6 presents the temperature variation of the CN–$H_2(j = 0)$ rate coefficients for selected $N = 2, j, F \to N' = 1, j', F'$ transitions. Table 1 shows the hyperfine-resolved CN–$H_2(j = 0)$ rate coefficients for $N = 3, j, F \to N' = 2, j', F'$ transitions at 50 K.

The discussion about the hyperfine propensity rules implies to distinguish $\Delta j = \Delta N$ and $\Delta j \neq \Delta N$ transitions. For $\Delta j = \Delta N$ transitions, we have a strong propensity rule in favour of $\Delta j = \Delta F$ transitions; the propensity rule is also more pronounced when the N quantum number increases. This trend is the usual trend for

[1] The HIBRIDON package was written by M. H. Alexander, D. E. Manolopoulos, H.-J. Werner and B. Follmeg, with contributions by P. F. Vohralik, D. Lemoine, G. Corey, R. Gordon, B. Johnson, T. Orlikowski, A. Berning, A. Degli-Esposti, C. Rist, P. Dagdigian, B. Pouilly, G. van der Sanden, M. Yang, F. de Weerd, S. Gregurick, J. Kłos and F. Lique. http://www2.chem.umd.edu/groups/alexander/

[2] http://www.strw.leidenuniv.nl/~moldata

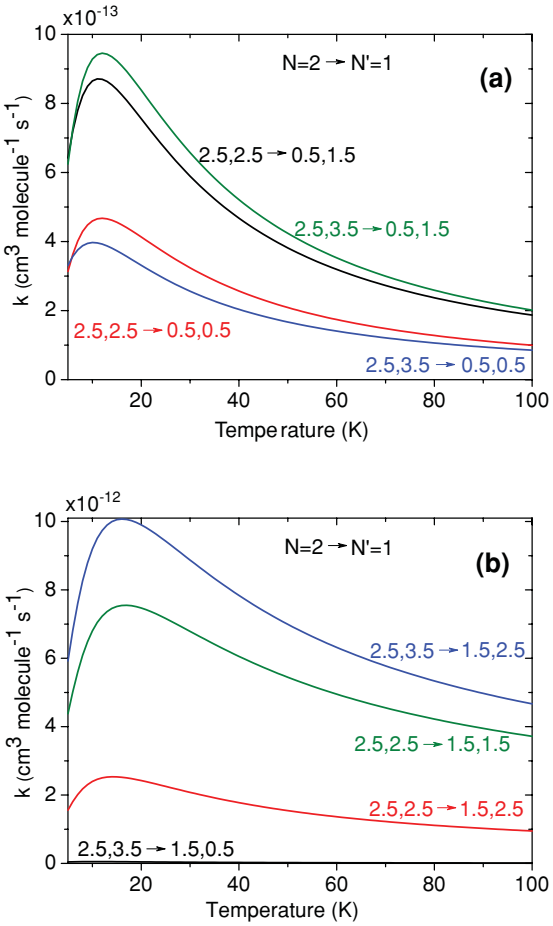

Figure 6. Temperature variation of the hyperfine-resolved CN–$H_2(j = 0)$ rate coefficients for $N = 2, j, F \rightarrow N' = 1, j', F'$ transitions. Panel (a) corresponds to $\Delta j = \Delta N$ transitions. Panel (b) corresponds to $\Delta j \neq \Delta N$ transitions.

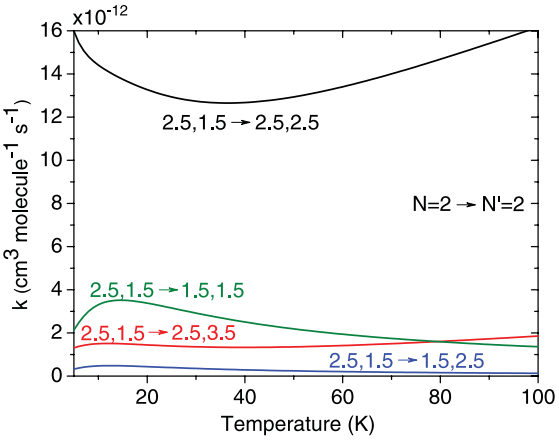

Figure 7. Temperature variation of the hyperfine-resolved CN–$H_2(j = 0)$ rate coefficients for $N = 2, j, F \rightarrow N' = 2, j', F'$ transitions.

open-shell molecules (Alexander & Dagdigian 1985; Corey & Alexander 1988) and was previously observed in the case of CN–He collisions (Lique & Kłos 2011). For $\Delta j \neq \Delta N$ transitions, no clear propensity rules can be extracted. Two rules seem to govern the transitions: the rate coefficients show propensity in favour of $\Delta j = \Delta F$ transitions and the final distribution seems to be proportional to the degeneracy $(2F' + 1)$ of the final hyperfine level. For example, for $N = 3, j = 3.5, F \rightarrow N' = 2, j' = 1.5, F'$ transitions at 50 K, one can see that when $F = 2.5$, all the final hyperfine levels from $N' = 2, j' = 1.5$ seem to be reasonably equally populated (competition between the two propensity rules), whereas, when $F = 4.5$, a propensity in favour of $F' = 2.5$ is observed [$\Delta j = \Delta F$ transitions and the highest degeneracy $(2F' + 1)$ for this state].

Fig. 7 presents the temperature variation in CN–$H_2(j = 0)$ rate coefficients for the 'quasi-elastic' $N = 2, j, F \rightarrow N' = 2, j', F'$ transitions.

First, one can note that the orders of magnitude of these 'quasi-elastic' rate coefficients are about the same order of magnitude than the pure inelastic rate coefficients. For transitions inside a rotational level N, we have clear propensity rules in favour of $\Delta j = 0$ transitions and $\Delta F = \pm 1$ that are about five times larger than the other ones. One can also note that the temperature variation of the $\Delta j = 0$ rate coefficients is not the same as all the other transitions. Indeed, these hyperfine rate coefficients were derived from the fine elastic ones ($\Delta N = \Delta j = 0$) that do not have the same variation with temperature than the inelastic ones.

4.3 Comparison with He rate coefficients

It is interesting to compare the present rate coefficients with those calculated for the CN–He collisions (Lique & Kłos 2011) using the same methodology as in the present work. By comparing the two sets of rate coefficients, we really analyse the effect of the different perturber masses and PES. Collisions with He are often assumed to model collisions with para-$H_2(j = 0)$, and it is generally assumed that rate coefficients with para-$H_2(j = 0)$ should be larger than He rate coefficients owing to the smaller collisional reduced mass, the scaling factor being 1.4 (Schöier et al. 2005). We have compared in Table 2, on a small sample, the CN–$H_2(j = 0)$ and CN–He rate coefficients at 10 and 30 K.

Table 1. Hyperfine-resolved CN–$H_2(j = 0)$ rate coefficients ($\times 10^{-12}$ cm^3 molecule^{-1} s^{-1}) for $N = 3, j, F \rightarrow N' = 2, j', F'$ transitions at 50 K.

			$j' = 1.5$			$j' = 2.5$	
		$F' = 0.5$	$F' = 1.5$	$F' = 2.5$	$F' = 1.5$	$F' = 2.5$	$F' = 3.5$
$j = 2.5$	$F = 1.5$	3.70	1.50	0.18	0.38	0.21	0.16
	$F = 2.5$	0.19	4.13	1.07	0.14	0.39	0.22
	$F = 3.5$	0.03	0.19	5.17	0.08	0.16	0.50
$j = 3.5$	$F = 2.5$	0.06	0.08	0.11	4.95	0.86	0.07
	$F = 3.5$	0.03	0.10	0.11	0.18	5.03	0.67
	$F = 4.5$	0.04	0.07	0.14	0.02	0.17	5.70

Table 2. Hyperfine-resolved CN–$H_2(j = 0)$ and CN–He rate coefficients ($\times\ 10^{-12}$ cm^3 molecule^{-1} s^{-1}) for $N = 3, j, F \rightarrow N', j', F'$ transitions at 10 and 30 K.

	Transition	10 K		30 K	
		He	H_2	He	H_2
$N' = 2$					
	$F = 1.5 \rightarrow F' = 3.5$	0.08	0.24	0.21	0.20
	$F = 2.5 \rightarrow F' = 3.5$	0.22	0.32	0.34	0.29
	$F = 3.5 \rightarrow F' = 3.5$	0.61	0.56	0.69	0.61
	$F = 1.5 \rightarrow F' = 2.5$	0.27	0.30	0.35	0.28
$j' = 2.5 \rightarrow j' = 2.5$	$F = 2.5 \rightarrow F' = 2.5$	0.42	0.39	0.47	0.45
	$F = 3.5 \rightarrow F' = 2.5$	0.17	0.24	0.26	0.21
	$F = 1.5 \rightarrow F' = 1.5$	0.47	0.38	0.49	0.44
	$F = 2.5 \rightarrow F' = 1.5$	0.18	0.20	0.23	0.19
	$F = 3.5 \rightarrow F' = 1.5$	0.04	0.12	0.10	0.10
$N' = 1$					
	$F = 2.5 \rightarrow F' = 2.5$	0.81	1.06	1.05	1.29
	$F = 3.5 \rightarrow F' = 2.5$	5.24	6.48	6.07	8.21
	$F = 4.5 \rightarrow F' = 2.5$	21.87	26.03	24.61	33.66
	$F = 2.5 \rightarrow F' = 1.5$	6.87	8.46	7.87	10.75
$j' = 3.5 \rightarrow j' = 1.5$	$F = 3.5 \rightarrow F' = 1.5$	16.70	19.62	18.70	25.56
	$F = 4.5 \rightarrow F' = 1.5$	0.21	0.46	0.38	0.44
	$F = 2.5 \rightarrow F' = 0.5$	14.44	17.03	16.16	22.14
	$F = 3.5 \rightarrow F' = 0.5$	0.18	0.44	0.31	0.41
	$F = 4.5 \rightarrow F' = 0.5$	0.04	0.05	0.09	0.06

As one can see, the scaling factor is clearly different from 1.4 and the ratio between the two sets of rate coefficients varies with the temperature and with the transition considered. The agreement seems better at 30 K than at 10 K. The very low collisional energies cross-sections are very sensitive to the shape and well depth of the PES and it is not surprising to see significant differences between the two collisional systems at 10 K. Overall, the CN–H_2/CN–He ratio varies between 1 and 3. The difference can be simply explained by checking the radial dependence of the potential expansion coefficients $V_\lambda(R)$ (see Fig. 3). The CN–$H_2(j = 0)$ radial coefficients are larger than those of CN–He PES, and this simply explains that the CN–$H_2(j = 0)$ rate coefficients are, overall, larger than those of CN–He ones. This comparison confirms that accurate rate coefficients with para-$H_2(j = 0)$ could not be obtained at very low temperature ($T < 10$ K) from rate coefficients with He but seems to indicate that, at higher temperature, rate coefficients with para-$H_2(j = 0)$ may be estimated from rate coefficients with He using a simple scaling factor corresponding to the reduced mass ratio.

5 CONCLUSION

We have used quantum scattering calculations to investigate rotational energy transfer in collisions of CN($X^2\Sigma^+$) with H_2 molecule in its ground rotational state. The calculations are based on a new, highly correlated 4D PES averaged over H_2 orientation. Fine- and hyperfine-state-resolved rate coefficients were determined for temperatures ranging from 5 to 100 K.

For fine-structure-resolved rate coefficients, one can see strong propensity rules in favour of $\Delta j = \Delta N$ transitions. For hyperfine-structure-resolved rate coefficients, the collisions exhibit strong propensity rules in favour of $\Delta j = \Delta F$ transitions for $\Delta j = \Delta N$ transitions. There is no notable propensity for the other transitions. It is important to specify that the rate coefficients presented here are not independent of the initial hyperfine level and not proportional to the degeneracy ($2F' + 1$) of the final hyperfine level. These important results show that the M_J randomizing limit method of Alexander & Dagdigian (1985) cannot be used for such a system.

The comparison of the new CN–$H_2(j = 0)$ rate coefficients with those of CN–He shows that important differences exist, especially at low temperature. Hence, the CN–H_2 rate coefficients have to be used for observation interpretations and we expect that their use will help us significantly in the interpretation of the CN emission lines observed with current and future telescopes.

Finally, we plan to extend the present calculations to calculation with para- and ortho-H_2 in order to provide accurate CN rate coefficients for higher temperature.

ACKNOWLEDGMENTS

We acknowledge Mohamed Jorfi for preliminary calculations. We acknowledge Millard Alexander and Paul Dagdigian for helpful discussions. This research was supported by the CNRS national programme 'Physique et Chimie du Milieu Interstellaire'. JK is grateful for financial support from the US National Science Foundation, Grant CHE-0848110, to M. H. Alexander.

REFERENCES

Adams W. S., 1941, ApJ, 93, 11
Agúndez M., Goicoechea J. R., Cernicharo J., Faure A., Roueff E., 2010, ApJ, 713, 662
Alexander M., 1982, J. Chemical Phys., 76, 3637
Alexander M. H., Dagdigian P. J., 1985, J. Chemical Phys., 83, 2191
Alexander M. H., Davis S. L., 1983, J. Chemical Phys., 79, 227
Alexander M., Smedley J. E., Corey G. C., 1986, J. Chemical Phys., 84, 3049
Balucani N., Asvany O., Huang L. C. L., Lee Y. T., Kaiser R. I., Osamura Y., Bettinger H. F., 2000, ApJ, 545, 892
Boys S. F., Bernardi F., 1970, Molecular Phys., 19, 553
Coletti C., Billing G. D., 2000, J. Chemical Phys., 113, 11101
Corey G. C., Alexander M. H., 1988, J. Chemical Phys., 88, 6931
Dumouchel F., Kłos J., Lique F., 2011, Phys. Chemistry Chemical Phys., 13, 8204
Falgarone E., Troland T. H., Crutcher R. M., Paubert G., 2008, A&A, 487, 247
Fuente A., Martin-Pintado J., Gaume R., 1995, ApJ, 442, L33
Green S., 1975, J. Chemical Phys., 62, 2271
Guillon G., Stoecklin T., 2012, MNRAS, 420, 579
Hakobian N. S., Crutcher R. M., 2011, ApJ, 733, 6
Hily-Blant P., Walmsley M., Pineau Des Forêts G., Flower D., 2008, A&A, 480, L5
Huber K. P., Herzberg G., 1979, Molecular Spectra and Molecular Structure IV. Constants of Diatomic Molecules. Van Nostrand Reinhold, New York
Kaledin A. L., Heaven M. C., Bowman J. M., 1999, J. Chemical Phys., 110, 10380
Kłos J., Lique F., 2008, MNRAS, 390, 239
Knowles P. J., Hampel C., Werner H.-J., 1993, J. Chemical Phys., 99, 5219
Knowles P. J., Hampel C., Werner H.-J., 2000, J. Chemical Phys., 112, 3106
Lique F., 2010, J. Chemical Phys., 132, 044311
Lique F., Faure A., 2012, J. Chemical Phys., 136, 031101
Lique F., Kłos J., 2008, J. Chemical Phys., 128, 034306
Lique F., Kłos J., 2011, MNRAS, 413, L20
Lique F., Senent M.-L., Spielfiedel A., Feautrier N., 2007, J. Chemical Phys., 126, 164312
Lique F., Toboła R., Kłos J., Feautrier N., Spielfiedel A., Vincent L. F. M., Chałasiński G., Alexander M. H., 2008, A&A, 478, 567
Lique F., van der Tak F. F. S., Kłos J., Bulthuis J., Alexander M. H., 2009, A&A, 493, 557

Lique F., Spielfiedel A., Feautrier N., Schneider I. F., Kłos J., Alexander M. H., 2010, J. Chemical Phys., 132, 024303
McCurdy C. W., Miller W. H., 1977, J. Chemical Phys., 67, 2488
McKellar A., 1940, PASP, 52, 187
Milam S. N., Woolf N. J., Ziurys L. M., 2009, ApJ, 690, 837
Schöier F. L., van der Tak F. F. S., van Dishoeck E. F., Black J. H., 2005, A&A, 432, 369
Smith I. W. M., 1980, Kinetics and Dynamics of Elementary Gas Reactions. Butterworths, London
Ter Horst M. A., Schatz G. C., Harding L. B., 1996, J. Chemical Phys., 105, 558
Truong-Bach, Nguyen-Q-Rieu, Omont A., Olofsson H., Johansson L. E. B., 1987, A&A, 176, 285
Werner H.-J., Follmeg B., Alexander M. H., Lemoine D., 1989, J. Chemical Phys., 91, 5425
Werner H.-J. et al., 2010, MOLPRO, Version 2010.1, A Package of Ab Initio Programs
Wernli M., Valiron P., Faure A., Wiesenfeld L., Jankowski P., Szalewicz K., 2006, A&A, 446, 367
Williams H. L., Mass E. M., Szalewicz K., Jeziorski B., 1995, J. Chemical Phys., 103, 7374
Woon D. E., Dunning T. H., 1994, J. Chemical Phys., 100, 2975
Zhang D. H., Lee S., 2000, J. Chemical Phys., 112, 203

This paper has been typeset from a TEX/LATEX file prepared by the author.